



Discovery of benzimidazole-based *Leishmania mexicana* cysteine protease CPB2.8 Δ CTE inhibitors as potential therapeutics for leishmaniasis

Laura De Luca¹ | Stefania Ferro¹ | Maria Rosa Buemi¹ | Anna-Maria Monforte¹ |
Rosaria Gitto¹ | Tanja Schirmeister² | Louis Maes³ | Antonio Rescifina⁴  |
Nicola Micale¹ 

¹Department of Chemical, Biological, Pharmaceutical and Environmental Sciences, University of Messina, Messina, Italy

²Institute of Pharmacy and Biochemistry, University of Mainz, Mainz, Germany

³Laboratory of Microbiology, Parasitology and Hygiene (LMPH), University of Antwerp, Antwerp, Belgium

⁴Department of Drug Sciences, University of Catania, Catania, Italy

Correspondence

Nicola Micale, Department of Chemical, Biological, Pharmaceutical and Environmental Sciences, University of Messina, Messina, Italy.
Email: nmicale@unime.it

Chemotherapy is currently the only effective approach to treat all forms of leishmaniasis. However, its effectiveness is severely limited due to high toxicity, long treatment length, drug resistance, or inadequate mode of administration. As a consequence, there is a need to identify new molecular scaffolds and targets as potential therapeutics for the treatment of this disease. We report a small series of 1,2-substituted-1*H*-benzo[*d*]imidazole derivatives (**9a–d**) showing affinity in the submicromolar range ($K_i = 0.15\text{--}0.69\ \mu\text{M}$) toward *Leishmania mexicana* CPB2.8 Δ CTE, one of the more promising targets for antileishmanial drug design. The compounds confirmed activity in vitro against intracellular amastigotes of *Leishmania infantum* with the best result being obtained with derivative **9d** ($\text{IC}_{50} = 6.8\ \mu\text{M}$), although with some degree of cytotoxicity ($\text{CC}_{50} = 8.0\ \mu\text{M}$ on PMM and $\text{CC}_{50} = 32.0\ \mu\text{M}$ on MCR-5). In silico molecular docking studies and ADME-Tox properties prediction were performed to validate the hypothesis of the interaction with the intended target and to assess the drug-likeness of these derivatives.

KEYWORDS

antileishmanial agents, benzimidazole derivatives, docking studies, in silico profiling, *Leishmania mexicana* CPB2.8

1 | INTRODUCTION

Human leishmaniasis is one of the vector-borne tropical infectious diseases with a high rate of morbidity and mortality worldwide, predominantly in endemic areas of developing countries.^[1] The clinical spectrum ranges from the most common and usually self-resolving cutaneous form to a disfiguring form affecting mucous membranes predominantly those of nose and mouth, and even to the most severe visceral form wherein the parasites invade especially liver and spleen. The latter form is fatal in the absence of a timely chemotherapeutic treatment.^[2] Despite several drug discovery efforts

that have been made in the recent past to counter the progression of this disease, the current armamentarium of effective and safe antileishmanial drugs remains quite inadequate. Pentavalent antimonials (i.e. meglumine antimoniate and sodium stibogluconate) are old and toxic drugs administered intramuscularly that still constitute, for a large part, the first-line of intervention. Liposomal amphotericin B, pentamidine salts, paromomycin sulfate, and oral miltefosine are the available second-line drugs in case of antimonial treatment failure.^[3] As for antimonials, these second-line drugs also have several drawbacks including toxicity, high costs, long-term treatments and repeated doses, emergence of resistance, and

need of constant medical care (which is difficult to afford in areas strongly related to poverty and lack of health services). In this scenario and in the absence of an effective vaccine, the identification of new targets and the development of new antileishmanial agents remain of primary importance.^[4] In this regard, the *Leishmania* parasite expresses high levels of several classes of cysteine proteases (CPs) belonging to the papain family whose activity has been recognized as essential for parasite survival and infectivity to the mammalian host.^[5] Among these CPs, cysteine proteases group B (CPBs) of *Leishmania mexicana* have been identified as virulence factors and putative druggable targets.^[6] In particular, the isoform CPB2.8, which is a typical cathepsin-L-like endopeptidase endowed also with carboxydipeptidase activity,^[7] remains relatively unexplored. As only few reports describe specific inhibitors of *L. mexicana* CPB2.8 Δ CTE (the recombinant form of the isoform CPB2.8 expressed without the C-terminal extension). These include peptide-based inhibitors bearing an electrophilic warhead that covalently traps the catalytic thiolate such as dipeptidyl vinyl sulfone **1**, dipeptidyl α -keto heterocycles **2** and aziridinyl peptides (e.g. **3**),^[8–12] semicarbazone **4**, thiosemicarbazones **5**, triazine nitrile **6**,^[13] natural compounds (e.g. morelloflavones **7**),^[14,15] and a decorated fused benzo[*b*]thiophene inhibitor **8** acting through a time-dependent bimodal mechanism of action (Figure 1).^[16]

In our ongoing search for novel antileishmanial agents that might specifically target *L. mexicana* CPB2.8 Δ CTE,^[16–18] we have made a screening campaign on our in-house database CHIME 1.6 containing compounds synthesized and stocked in laboratory. Therefore, we have initially selected small compounds possessing the benzimidazole or imidazole ring as common chemical feature. The idea of testing these derivatives arose from literature data indicating that compounds containing an indole/benzimidazole scaffold showed potent anti-*Leishmania* properties with no specific insights about the possible targets. This extensive list of indole-based compounds contains indolylquinolines,^[19] azoles,^[20] alkaloids,^[21] indole-2-hydrazones,^[22] indole-2-carboxamides,^[23] C3-mono-functionalized oxindoles,^[24] and thiophene-indole hybrids.^[25] Some of selected small compounds have been previously studied as potential HIV-1 non-nucleoside reverse transcriptase inhibitors (NNRTIs)^[26] as well as negative allosteric modulators of GluN2B-containing NMDA receptors in mammalian central nervous system.^[27–32]

As a result of our preliminary screening of a set of twelve compounds, four 1,2-disubstituted-1*H*-benzo[*d*]imidazole derivatives (i.e. **9a–d**; Figure 2) turned out to be active against the listed intended target. The remaining eight indole derivatives I–VIII proved to be low inhibitors of *L. mexicana* CPB2.8 Δ CTE at 20 μ M concentration (see Appendix S1).

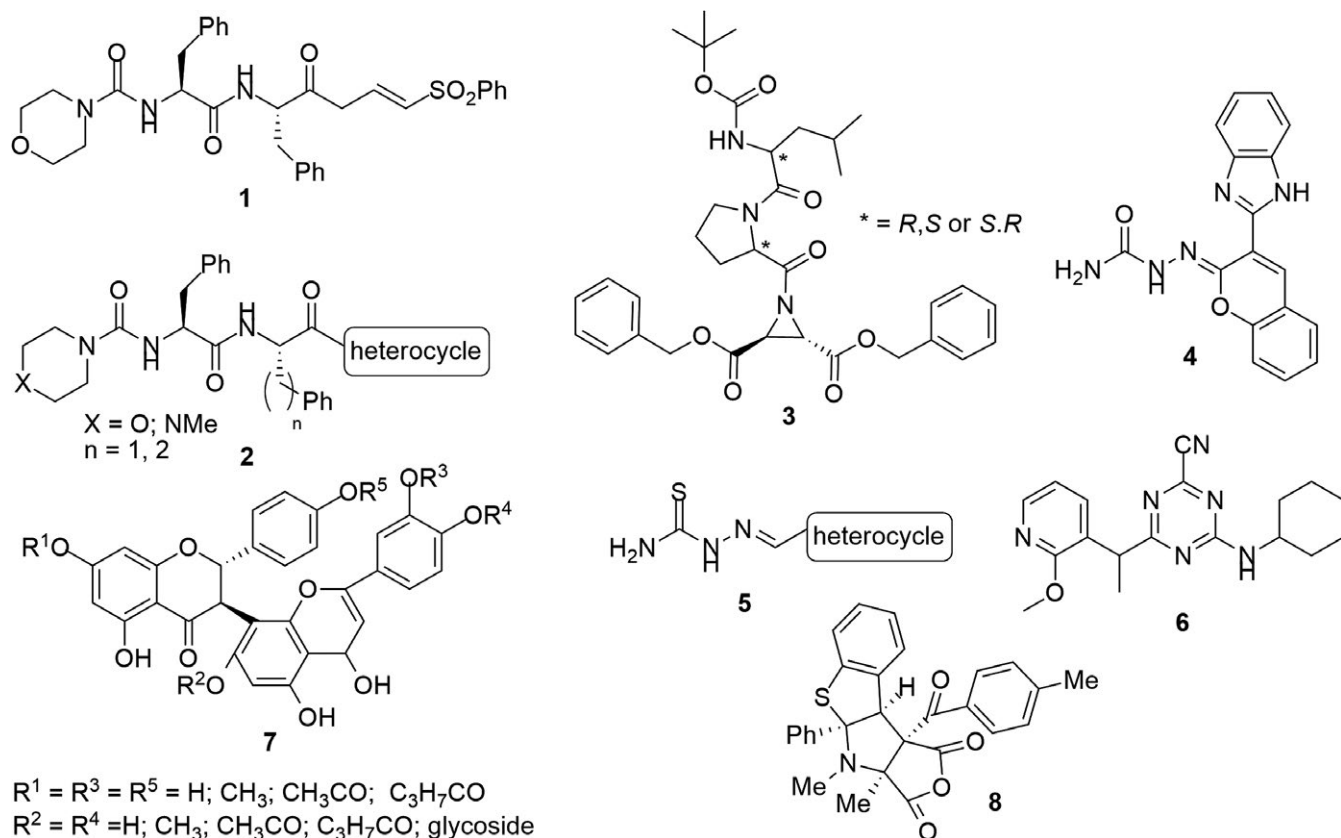


FIGURE 1 Chemical structures of known *Leishmania mexicana* CPB2.8 Δ CTE inhibitors

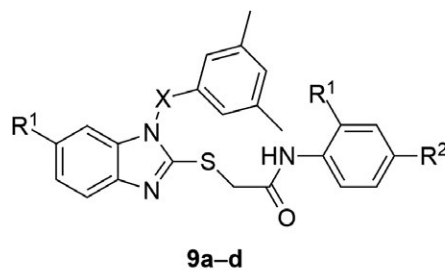


FIGURE 2 Chemical structures of the 1,2-disubstituted-1*H*-benzo[*d*]imidazole derivatives tested against *Leishmania mexicana* CPB2.8ΔCTE

	X	R ¹	R ²
9a	–SO ₂	H	H
9b	–SO ₂	H	CO ₂ Me
9c	–SO ₂	Cl	CO ₂ Me
9d	–CH ₂	Cl	CO ₂ Me

2 | METHODS AND MATERIALS

2.1 | Chemistry

2.1.1 | General information

Characterization of each new intermediate and final compound (i.e. melting points, elemental analyses and NMR spectra) were determined by means of equipments previously reported by our group, as well as materials and purification methods.^[27]

2.1.2 | General procedures for the synthesis of *N*-(2-nitrophenyl)-benzenesulfonamides (10,11) and *N*-substituted-2-nitroaniline (12)

Derivatives **10–12** were prepared following the synthetic procedures previously reported by us.^[26–28] A mixture of anhydrous sodium hydride (5 mmol) and 2-nitroaniline (138 mg, 1 mmol) or 5-chloro-2-nitroaniline (173 mg, 1 mmol) in DMF (5 ml) was stirred for 10 min at 0°C and then 3,5-dimethylbenzyl bromide (597 mg, 3 mmol) or 3,5-dimethylbenzenesulfonyl chloride (614 mg, 3 mmol) was added. When the reaction was completed (2–6 hr), a saturated NaHCO₃ aqueous solution was added. The mixture was extracted with dichloromethane (3 × 10 ml) and dried over Na₂SO₄. After removal of the solvent under reduced pressure, the residue was triturated by treatment with diethyl ether and crystallized from ethanol.

Spectral data of compounds **10**,^[26] **11**,^[28] and **12**^[27] are in accordance with the literature.

2.1.3 | General procedures for the synthesis of *N*-(2-aminophenyl)-benzene sulfonamides (13,14) and *N*₁-(substituted-benzyl)-2-amino aniline (15)

Derivatives **13–15** were prepared following the synthetic procedures previously reported by us.^[26–28] The mixture of *N*-substituted-2-nitroanilines (1 mmol) or *N*-(2-nitrophenyl)-benzenesulfonamides (1 mmol) in HCl conc. (5 ml) and

EtOH (7 ml) was stirred vigorously, and then, zinc dust (2.18 g, 33 mmol) was added in several portions at room temperature. When the addition was completed, the reaction was refluxed (80°C) for 1 hr. Then, the resulting mixture was cooled, made alkaline with NaOH 2N aqueous solution, and extracted with ethyl acetate (3 × 10 ml). The organic phases were collected, washed with water, dried over Na₂SO₄, and evaporated. The residue was crystallized from ethanol or purified by column flash chromatography using cyclohexane/AcOEt as eluent.

Spectral data of compounds **13**,^[26] **14**,^[28] and **15**^[27] are in accordance with the literature.

2.1.4 | General procedures for the synthesis of 1-(3,5-dimethylbenzyl)-1,3-dihydro-2*H*-benzimidazol-2-one (16) and 1-(3,5-dimethylphenylsulfonyl)-1,3-dihydro-2*H*-benzimidazol-2-ones (17,18)

Derivatives **16–18** were prepared following the synthetic procedures previously reported by us.^[26–28] To a solution of *N*₁-(substituted-benzyl)-2-amino aniline (1 mmol) or *N*-(2-aminophenyl)-benzenesulfonamides (1 mmol) in pyridine (10 ml) 1,1'-thiocarbonyldiimidazole (250 mg, 1.4 mmol) was added at room temperature and the resulting mixture was maintained under stirring for 1 hr. After this time, distilled water was added to quench the reaction and the precipitate was filtered off to give the desired products after cooling.

Spectral data of compounds **16**,^[26] **17**,^[28] and **18**^[27] are in accordance with the literature.

2.1.5 | General procedures for the synthesis of 2-chloro-*N*-phenylacetamides (19–21)

Derivatives **19–21** were prepared following the synthetic procedures previously reported by us.^[26,33] *N,N*-Diisopropylethylamine (175 μl, 1 mmol) and then chloroacetyl chloride (78 μl, 1 mmol) were added dropwise to a solution of suitable substituted anilines (1 mmol) in dichloromethane (5 ml). The mixture was stirred for 1 hr at room

temperature. Successively, the reaction was quenched with a saturated NaHCO₃ aqueous solution. The reaction mixture was extracted with ethyl acetate (3 × 10 ml), dried over Na₂SO₄, and evaporated under reduced pressure. The residue was crystallized from ethanol.

2-Chloro-*N*-phenylacetamide (19)

Yield 65%; m.p.: 115–117°C. ¹H NMR (DMSO-*d*₆): 4.23 (s, 2H, CH₂); 7.07 (m, 1H, ArH); 7.31 (m, 2H, ArH); 7.56 (m, 2H, ArH); 10.29 (bs, 1H, NH). Anal. Calcd for C₈H₈ClNO: C, 56.65; H, 4.75; N, 8.26. Found: C, 56.72; H, 4.79; N, 8.30.

Spectral data of compounds **20** and **21** are in accordance with the literature.^[26,33]

2.1.6 | General procedure for the synthesis of 1,2-substituted-1H-benzo[d]imidazole derivatives 9a–d

Derivatives **9a–d** were prepared following the synthetic procedures previously reported by us.^[26] A solution of 1-(3,5-dimethylbenzyl or 3,5-dimethylphenylsulfonyl)-1H-benzo[d]imidazole-2(3H)-thione derivative (1 mmol) (**16–18**) in DMF (3 ml), anhydrous potassium carbonate (138 mg, 1 mmol), and the appropriate 2-chloro-*N*-phenylacetamide (1 mmol) (**19–21**) was stirred at room temperature for 1.5 hr. The reaction was quenched by the addition of saturated NaHCO₃ aqueous solution and the mixture was extracted with ethyl acetate (3 × 10 ml). After removal of the solvent under reduced pressure, the residue was crystallized by treatment with ethanol or purified by column flash chromatography using cyclohexane/AcOEt as eluent.

2-(1-(3,5-Dimethylphenylsulfonyl)-1H-benzo[d]imidazol-2-ylthio)-*N*-phenylacetamide (9a)

Yield 61%; m.p.: 159–161°C. ¹H NMR (DMSO-*d*₆): 2.32 (s, 6H, (CH₃)₂); 4.35 (s, 2H, CH₂); 7.01–7.06 (m, 1H, ArH); 7.26–7.31 (m, 4H, ArH); 7.40 (s, 1H, ArH); 7.55–7.57 (m, 3H, ArH); 7.80–7.88 (m, 3H, ArH); 10.38 (bs, 1H, NH). Anal. Calcd for C₂₃H₂₁N₃O₃S₂: C, 61.18; H, 4.69; N, 9.31. Found: C, 61.32; H, 4.79; N, 9.21.

Spectral data of methyl-4-(2-(1-(3,5-dimethylphenylsulfonyl)-1H-benzo[d]imidazol-2-ylthio)acetamido) benzoate (**9b**), methyl 3-chloro-4-(2-(6-chloro-1-(3,5-dimethylphenylsulfonyl)-1H-benzo[d]imidazol-2-ylthio)acetamido)benzoate (**9c**) and methyl 3-chloro-4-(2-(6-chloro-1-(3,5-dimethylbenzyl)-1H-benzo[d]imidazol-2-ylthio)acetamido)benzoate (**9d**) are in accordance with the literature.^[26,33] Data of elemental analysis for the last three resynthesized compounds are the following: Anal. Calcd for C₂₅H₂₃N₃O₅S₂ (**9b**): C, 58.92; H, 4.55; N, 8.25. Found: C, 58.98; H, 4.59; N, 8.20. Anal. Calcd for C₂₅H₂₁Cl₂N₃O₅S₂ (**9c**): C, 51.91; H, 3.66; N, 7.26. Found: C, 52.00; H, 3.69; N, 7.20. Anal. Calcd for C₂₆H₂₃Cl₂N₃O₅S

(**9d**): C, 59.09; H, 4.39; N, 7.95. Found: C, 59.17; H, 4.41; N, 7.92.

2.2 | Biological activity

2.2.1 | Enzyme assays

Recombinant *L. mexicana* cysteine protease CPB2.8ΔCTE was expressed and purified as previously described,^[34,35] whereas human cathepsins B and L were purchased from Calbiochem. The initial screening of benzimidazole and indole derivatives against the parasite enzyme was performed at 20 μM concentration according to well-established methods previously reported.^[16] Compounds showing at least 50% inhibition (i.e. **9a–d**) were subjected to detailed follow-up assays against the target and cross-reactivity screening against the above-mentioned cathepsins.^[16,36]

2.2.2 | In vitro amastigote assay

The in vitro anti-*Leishmania* assay of **9a–d** was performed as previously described by using *Leishmania infantum* MHOM/MA (BE)/67 intracellular amastigotes collected from the spleen of an infected donor hamster and used to infect primary peritoneal mouse macrophages.^[37] Miltefosine was included as reference drug.

2.2.3 | Cytotoxicity assays

Cytotoxicity assays were performed both on MRC5_{SV2} and PMM cells according to procedures previously reported.^[37] Tamoxifen was included as the reference drug.

2.3 | Docking

2.3.1 | Preparation of ligands

The 3D structures of ligands were built using Gabedit (2.4.8) software,^[38] and all geometries were fully optimized, in the same software, with the semiempirical PM6 Hamiltonian^[39] implemented in MOPAC2016 (17.130W).^[40]

2.3.2 | Molecular dynamics simulations

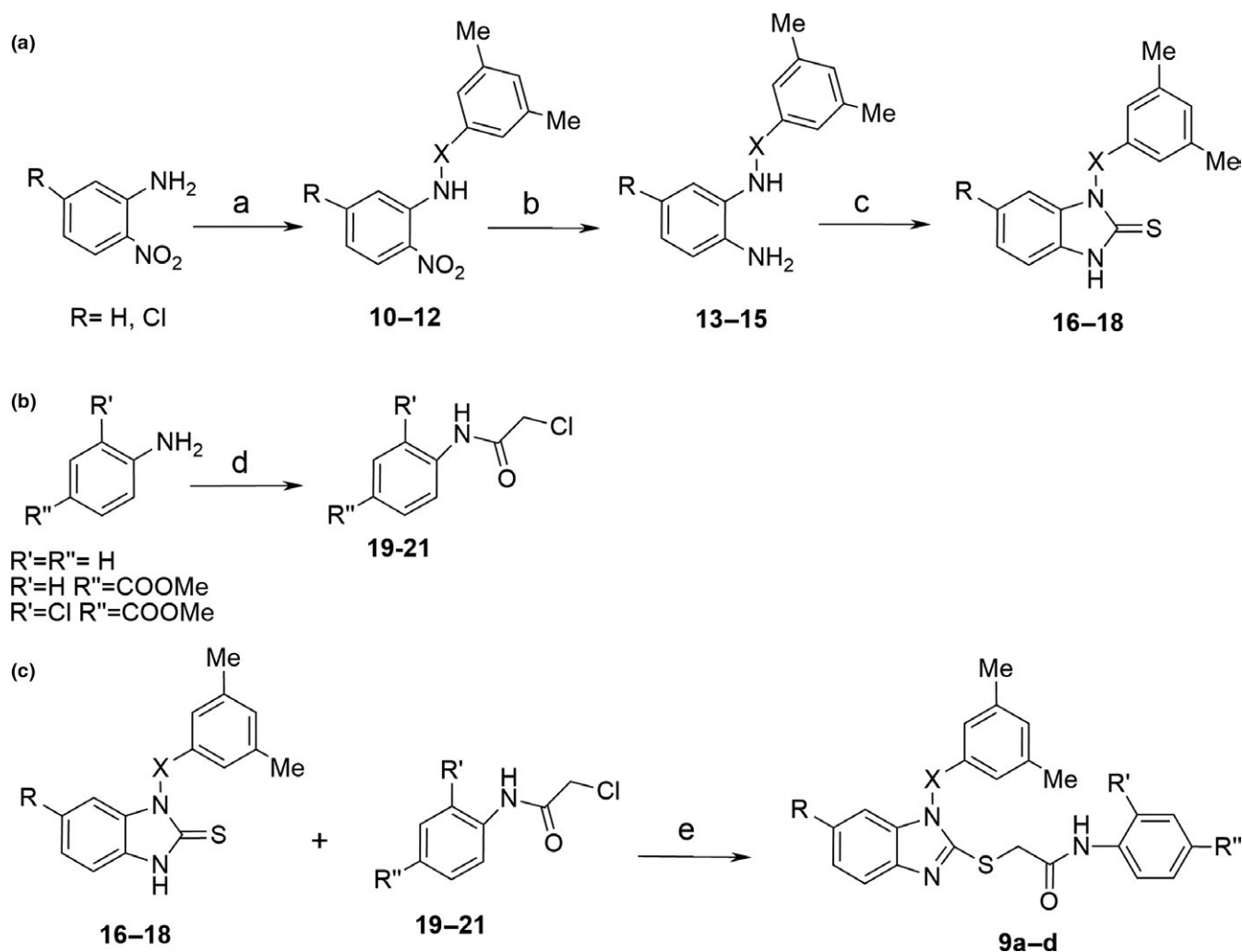
The molecular dynamics simulations of the mature *L. mexicana* CPB2.8ΔCTE/ligand complexes (based on the PDBs prepared as described above) were performed with the YASARA Structure package (17.4.17).^[41] A periodic simulation cell with boundaries extending 10 Å from the surface of the complex was employed. The box was filled with water, with a maximum sum of all bumps per water of 1.0 Å, and a density of 0.997 g/ml with explicit solvent. YASARA's pK_a utility was used to assign pK_a values at

pH 7.2,^[42] and the cell was neutralized with NaCl (0.9% by mass); in these conditions, ligands **9** result protonated at pyrrolidinic *N*-Me. Water was deleted to readjust the solvent density to 0.997 g/ml. The YASARA2 force field was used with long-range electrostatic potentials calculated with the Particle Mesh Ewald (PME) method, with a cutoff of 8.0 Å.^[43–45] The ligand force field parameters were generated with the AutoSMILES utility,^[46] which employs semiempirical AM1 geometry optimization and assignment of charges, followed by the assignment of the AM1BCC atom and bond types with refinement using the RESP charges, and finally the assignments of general AMBER force field atom types. Optimization of the hydrogen bond network of the various enzyme–ligand complexes was obtained using the method established by Hooft et al.,^[47] to address ambiguities arising from multiple side chain conformations and protonation states that are not well resolved in the electron density.^[48] A short MD was run on the solvent only. The entire system was then energy minimized using first a steepest descent minimization to remove conformational

stress, followed by a simulated annealing minimization until convergence (<0.01 kcal/mol Å). The MD simulation was then initiated, using the NVT ensemble at 298 K, and integration time steps for intramolecular and intermolecular forces every 1.25 fs and 2.5 fs, respectively. The MD simulation was stopped after 40 ns and, on the averaged structure of the last 3 ns frames, a second cycle of energy minimization, identical to the first, was applied.

2.3.3 | Docking protocol

Macromolecules and ligands, as obtained after MD simulation and energy minimization, were prepared with Vega ZZ (3.1.1)^[49] assigning Gasteiger charges to the protein and AM1BCC ones to the ligand. Fine docking was performed by applying the Lamarckian genetic algorithm (LGA) implemented in AutoDock 4.2.6.^[50] The ligand-centered maps were generated by the program AutoGrid (4.2.6) with a spacing of 0.375 Å and dimensions that encompass all atoms extending 5 Å from the surface of the ligand. All of



SCHEME 1 Reagents and conditions: (a) DMF, NaH, rt, 2–6 hr (b) Zn/HCl, EtOH, 80°C, 1 hr; (c) TCDI, pyridine, rt, 1 hr; (d) chloroacetyl chloride, DIPEA, CH₂Cl₂, rt, 1 hr; (e) K₂CO₃, DMF, rt, 1.5 hr

the parameters were inserted at their default settings. In the docking tab, the macromolecule and ligand are selected, and GA parameters are set as $ga_runs = 100$, $ga_pop_size = 150$, $ga_num_evals = 20,000,000$, $ga_num_generations = 27,000$, $ga_elitism = 1$, $ga_mutation_rate = 0.02$, $ga_crossover_rate = 0.8$, $ga_crossover_mode = two\ points$, $ga_cauchy_alpha = 0.0$, $ga_cauchy_beta = 1.0$, number of generations for picking worst individual = 10.

Because no water molecule is directly involved in complex stabilization they were not considered in the docking process. All protein amino acidic residues were kept rigid, whereas all single bonds of ligands were treated as full flexible.

3 | RESULTS AND DISCUSSION

3.1 | Chemistry

The synthesis of the selected panel of 1,2-disubstituted-1*H*-benzo[*d*]imidazole derivatives **9a–d** was accomplished following a straightforward procedure developed in our laboratories^[26,33,51,52] and is depicted in Scheme 1. After obtaining the two main fragments *N*₁-aryl-1,3-dihydro-2*H*-benzimidazole-2-thiones (**16–18**) and 2-chloro-*N*-phenylacetamides (**19–21**) (Schemes 1a,b), both were condensed by reaction in dimethylformamide and in presence of K_2CO_3 (Scheme 1c) to yield the target compounds **9a–d**.

The final products **9a–d** were purified by recrystallization from ethanol or by column flash chromatography on silica gel to afford pure samples for biological assays. Analytical and spectral data (¹H NMR) of all synthesized compounds are in full agreement with the proposed structures.

3.2 | Biological activity

3.2.1 | Enzyme assays

Compounds **9a–d** were preliminarily screened against *L. mexicana* CPB2.8ΔCTE at a fixed 20 μM concentration to assess their ability to target the enzyme. Cross-reactivity assays against highly similar human cysteine proteases cathepsin-B (Cat-B) and cathepsin-L (Cat-L)

were performed in parallel under the same experimental conditions. An equivalent volume of DMSO was used as negative control, and Cbz-Phe-Arg-AMC was employed as the fluorogenic substrate. All compounds strongly inhibited the intended parasitic target (>90%) without significantly affecting (from “no inhibition” for Cat-B to a maximum of 20% of inhibition for Cat-L) the human counterparts (Table 1) pointing out a remarkable selectivity of the new “lead” structures. Hence, compounds **9a–d** were further evaluated against the parasite target by progress curve analysis (Figure 3: inhibition of CPB2.8ΔCTE by compound **9c**) using a continuous readout.^[53] As can be seen from the data in Table 1, the three compounds having the sulfone group as connection unit between the benzimidazole scaffold and the aryl group at its N1 (i.e. **9a–c**) showed IC₅₀ values in the submicromolar range, whereas the compound having the methylene group as connection unit at the same position (i.e. **9d**) turned out to be roughly one order of magnitude less potent. These results suggest that the electron-rich sulfone group may take part considerably to the binding network involved within the catalytic site of the enzyme, presumably as H-bond acceptor. In addition, the introduction of electron-withdrawing substituents to the phenyl ring of the 2-ylthioacetamide side chain of the benzimidazole core (e.g. **9a** vs. **9b**) positively affects the binding affinity toward the target, as well as the introduction of additional substituents with the same characteristics to the C6 position of the base scaffold (e.g. **9b** vs. **9c**).

3.2.2 | In vitro antileishmanial activity and cytotoxicity

Compounds **9a–d** were evaluated in vitro against intracellular amastigotes of *L. infantum* to establish whether any correlation exists between the inhibition of the target enzyme and the activity against the whole organism. Cytotoxicity assays were also performed on primary peritoneal mouse macrophages (PMM) and human fetal lung fibroblasts (MCR-5) to assess the selectivity. The in vitro profiling was carried out as previously described.^[54] The results point out that there is not a clear correlation between the activity against the selected *L. mexicana* CPB2.8ΔCTE target and the activity against the parasite (Table 2). The most

Compound	% inhibition at 20 μM			IC ₅₀ (μM)	K _i (μM) ^a
	CPB2.8ΔCTE	Cat-B	Cat-L		
9a	95.6 ± 0.5	n.i.	13.7 ± 2.0	0.68 ± 0.06	0.23 ± 0.02
9b	97.2 ± 0.4	n.i.	20.3 ± 3.5	0.54 ± 0.13	0.18 ± 0.04
9c	97.4 ± 0.6	n.i.	12.5 ± 2.1	0.45 ± 0.03	0.15 ± 0.01
9d	92.0 ± 0.9	12.8 ± 1.8	16.5 ± 2.2	2.06 ± 0.92	0.69 ± 0.31

n.i., no inhibition.

^aAssuming compounds are competitive inhibitors.

TABLE 1 Screening at 20 μM of **9a–d** against *Leishmania mexicana* CPB2.8ΔCTE. Human Cat-B and Cat-L were used in the counter assay to test the selectivity profile. IC₅₀ values include standard deviation from two independent experiments, each performed in duplicate. K_i ± SD values have been calculated using the Cheng-Prusoff equation

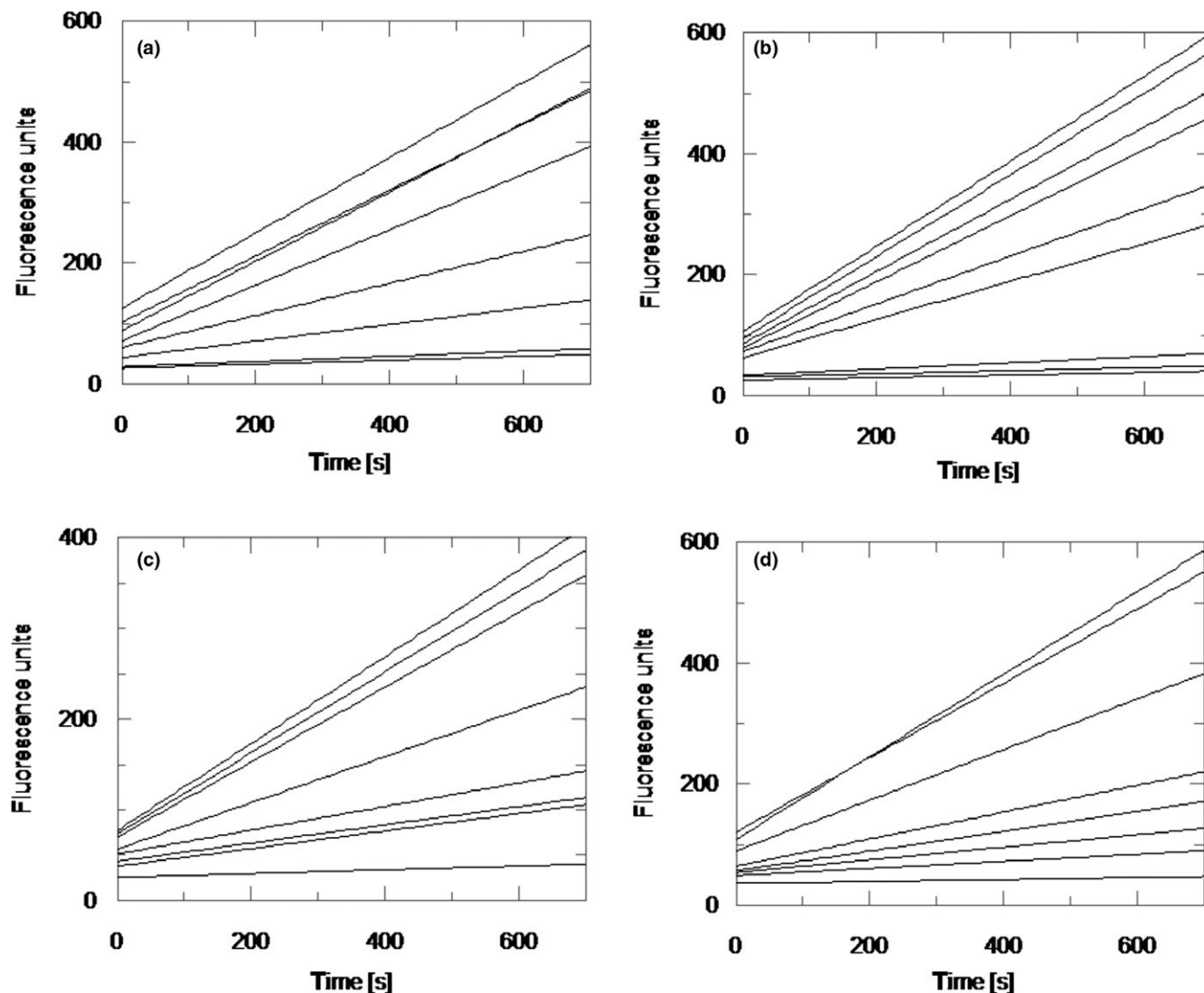


FIGURE 3 Progress curves of substrate hydrolysis in the presence of inhibitor **9c** (0, 0.25, 0.5, 1.0, 2.5, 5.0, 10.0 μM from top to bottom), continuously determined over a period of 10 min. Substrate: Cbz-Phe-Arg-AMC. Experiments were performed in duplicate. A representative graph is shown

potent compound in the cell-based assay turned out to be **9d**, with an IC_{50} value in the micromolar range (6.82 μM) comparable to that of the reference compound miltefosine (4.50 μM). The other three derivatives **9a–c**, which inhibit the molecular target more efficaciously than **9d**, showed fair activity (range 20–50 μM) against the whole organism. As the most relevant difference in terms of chemical structure between **9a–c** and **9d** is the sulfone group versus methylene group as connection unit at the N1 of the benzimidazole scaffold, we presume that one reason of this discrepancy in terms of activity could be the presence of the sulfone group that unfavorably (compared to the methylene group) may affect the diffusion through the biological barriers. A similar profile has been detected in the cytotoxicity assays against PMM and MRC-5 cells (Table 2). Indeed, the

TABLE 2 In vitro antileishmanial activity and cytotoxicity (IC_{50} μM and CC_{50} μM , respectively) of selected benzimidazole-based derivatives **9a–d**

Compound	<i>Leishmania infantum</i> ^a	PMM ^b	MCR-5 ^c
9a	50.8	>64.0	>64.0
9b	20.3	32.0	>64.0
9c	32.5	32.0	>64.0
9d	6.8	8.0	32.0
Tamoxifen	—	—	10.9
Miltefosine	4.5	—	—

^a*Leishmania infantum* MHOM/MA/67/ITMAP263.

^bPrimary peritoneal mouse macrophages.

^cHuman fetal lung fibroblast (MRC-5) cell line toxicity.

most active compound **9d** proved to be a more cytotoxic agent against PMM and MCR-5 when compared with inhibitors **9a–c**.

3.3 | Docking studies

To better rationalize the ligand–enzyme interactions, more accurate docking experiments were carried out utilizing the

TABLE 3 Calculated K_i and ligand efficiency (LE) values for compounds **9a–d**

Compound	Experimental K_i (nM)	Calculated K_i (nM)	N	LE
9a	230	383	31	0.28
9b	180	194	35	0.26
9c	150	136	37	0.25
9d	690	750	35	0.28

homology model of mature *L. mexicana* CPB2.8 Δ CTE that had been previously generated and validated.^[16]

Inactivation of a protease by an active-site directed irreversible inhibitor usually proceeds by the rapid formation of a noncovalent reversible enzyme–inhibitor complex (E-I), and successively in a slower chemical step, a covalent bond is formed with the enzyme to generate the enzyme–inhibitor adduct (E-I).^[55] As the test compounds do not contain an electrophilic group which could covalently react with the target enzyme, we conducted the study utilizing a sequence inherent to only the first stadium of enzyme recognition: (a) noncovalent docking of ligand upon mature *L. mexicana* CPB2.8 Δ CTE enzyme; (b) 25 ns of MD simulation of the best pose obtained for ligand-CPB2.8 Δ CTE complex, to accommodate the ligand; (c) noncovalent redocking of the complex obtained from the last 3 ns of MD simulation averaged frames. The above sequence has been appropriately

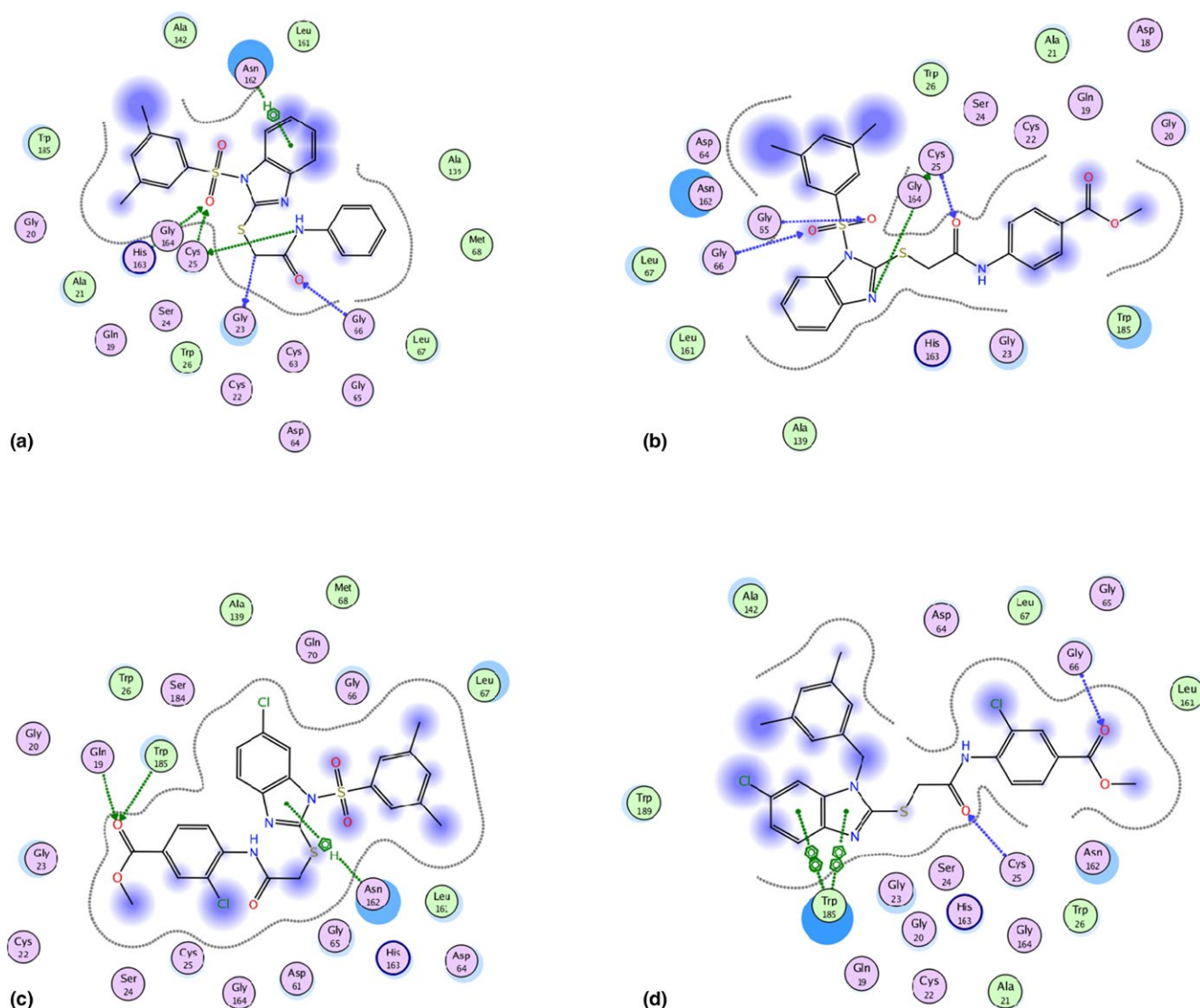


FIGURE 4 2D Schematic view of hydrophobic, hydrogen bond, π -H, and π - π interactions for compounds **9a–d**. From top left to bottom right [Colour figure can be viewed at wileyonlinelibrary.com]

TABLE 4 Calculated interaction energies for hydrogen bond interactions of compounds **9a–d** with CPB2.8ΔCTE

Compound	Ligand	Receptor	Interaction	Distance (Å)	<i>E</i> (kcal/mol) ^a
9a	N3	SG CYS25	H-donor	4.02	−1.7
	C4	O GLY23	H-donor	2.83	−0.8
	O1	N GLY66	H-acceptor	3.00	−3.1
	O17	SG CYS25	H-acceptor	3.11	−1.0
	O17	ND1 HIS163	H-acceptor	2.99	−5.9
	6-ring	CB ASN162	π–H	3.66	−0.6
9b	N13	SG CYS25	H-donor	3.37	−2.1
	O1	N CYS25	H-acceptor	3.14	−3.1
	O30	CA GLY65	H-acceptor	2.67	−0.7
	O31	N GLY66	H-acceptor	3.04	−2.7
9c	O11	NE2 GLN19	H-acceptor	2.82	−1.2
	O11	NE1 TRP185	H-acceptor	2.89	−3.8
	5-ring	CA ASN162	π–H	3.72	−1.4
9d	O1	N CYS25	H-acceptor	2.78	−5.7
	O34	N GLY66	H-acceptor	2.86	−2.0
	5-ring	5-ring TRP185	π–π	3.79	−0.0
	6-ring	5-ring TRP185	π–π	3.47	−0.0
	6-ring	6-ring TRP185	π–π	3.94	−0.0

^aCalculated by the analyze interactions subroutine present in YASARA software (v. 17.4.17, <http://www.yasara.org/>).

adapted from that previously used,^[16] which was shown to be effective in performing a suitable level of docking accuracy.

The calculated values of K_i obtained by the noncovalent redocking for compounds **9a–d** are reported in Table 3, and in all cases, they are in parallel with those obtained experimentally.

To avoid an over-scoring of the calculated energy of the database of the compounds, the “ligand efficiency” (LE) of all the molecular structures was calculated,^[56,57] taking into account the slight different molecular weight between the molecules and the cocrystallized ligand. In fact, an increase in the molecular weight may influence the amount of van der Waals interactions, representing an important factor for the calculations with docking software. The concept of ligand efficiency has recently emerged as a measure for lead compound selection.^[58,59] This parameter is useful and efficient for the prediction of the activity in the process of drug discovery. The ligand efficiency depends on the dimension of the ligand, as smaller ligands have a higher efficiency than the larger ligands. One of the causes behind this principle is the reduction in the area accessible to the ligand on increasing the size of the ligand. These considerations play an important role for the screening of compound databases. Ligand efficiency is calculated using the equation $LE = \Delta G_B/N$, where N is the number of nonhydrogen atoms.

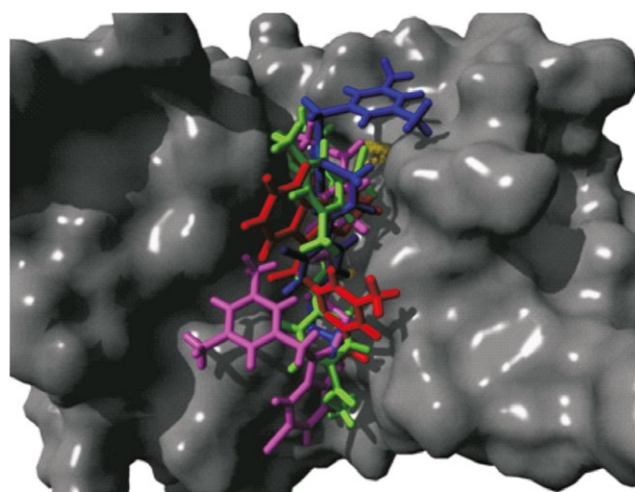


FIGURE 5 3D superposition of the best-docked pose for compounds **9a–d** (**a** in red, **b** in green, **c** in blue, and **d** in magenta) [Colour figure can be viewed at wileyonlinelibrary.com]

On this basis, we calculated the LE of our compounds and for the standard ligands (Table 3) from which it emerged that compounds **9a** and **9d** are a little more efficient than **9b** and **9c**.

The best-docked pose of compounds **9a–d** together with amino acid interactions in the binding pocket of the

TABLE 5 In silico Lipinski's rule of five parameters and drug-likeness of compounds **9a–d**^a

Compound	MW	Number of H-bond acceptors	Number of H-bond donors	log <i>P</i>	log <i>D</i> _{5.0}	log <i>D</i> _{7.4}	TPSA	Number of Lipinski's violations	Drug-likeness
9a	451.56	4	1	5.13	5.13	5.13	81.06	1	False
9b	509.60	5	1	5.13	5.13	5.13	107.36	2	False
9c	578.48	5	1	6.34	6.34	6.34	107.36	2	False
9d	528.45	3	1	7.36	7.34	7.36	73.22	2	False

^aChem for Excel (version 17.4.300.1589) was used for structure-property prediction and calculation, ChemAxon (<http://www.chemaxon.com>).

TABLE 6 Selected in silico ADME-Tox profiling of compounds **9a–d**^a

Compound	Absorption		Distribution		Toxicity		
	HIA (%)	In vitro Caco-2 cell permeability (nm/s)	In vitro PPB (%)	In vivo BBB penetration ($C_{\text{brain}}/C_{\text{blood}}$)	Ames test	Carcinogenicity in rat	Carcinogenicity in mouse
9a	96.97	21.48	100	0.51	Nonmutagen	Negative	Negative
9b	98.03	21.15	100	0.57	Nonmutagen	Negative	Positive
9c	97.82	11.92	100	0.93	Mutagen	Negative	Positive
9d	97.63	48.11	100	0.08	Nonmutagen	Negative	Negative

^aThe properties related to ADME were predicted using Pre-ADMET web-based application (<http://preadmet.bmdrc.kr>).

CPB2.8 Δ CTE is represented in Figure 4 as a 2D arrangement. Almost all interactions are due to hydrogen bond, although one π -H interaction for each of **9b** and **9c**, and three π - π interactions for **9d** are also proposed. The energies of these interactions have been reported in Table 4. Notably, all compounds explore a different interacting space on the enzymatic surface depending on substituents diversification; this is clearly evidenced in the 3D superposition of the best-docked poses reported in Figure 5.

3.4 | In silico profiling

ADME-Tox properties of compounds **9a–d** were investigated with the same criteria previously adopted by us, and the results of these preliminary in silico studies are reported in Tables 5 and 6. The “drug-likeness” of **9a–d** was searched for the Lipinski’s rule and for the standard ADME prediction, that is the human intestinal absorption (HIA), Caco-2 cell permeability, plasma protein binding (PPB), and blood–brain barrier (BBB) penetration. Ames mutagenic and carcinogenic potentials were calculated for the toxicity profiling.

The overview of the physicochemical properties reported in Table 5 indicates that compounds **9a–d** do not satisfy the whole Lipinski’s rule of five and that they cannot be considered at first sight “drug-like” according to Oprea’s descriptor-based scoring scheme.^[60] Nevertheless, compound **9a** shows only a single violation, viz. log *P*.

The in silico ADME results instead (Table 6) clearly indicate that compounds **9a–d** possess a promising oral availability (e.g. optimal HIA >95%; suboptimal Caco-2 cell permeability) and a strong plasma protein binding (PPB = 100%). Interestingly, compounds **9a–c** are supposed to moderately permeate the BBB (BBB penetration <1) unlike **9d** (BBB penetration = 0.08); as the penetration through BBB is not required for the treatment of leishmaniasis, compound **9d** turns out to be less likely to cause neurotoxicity. Finally, with the exception of compounds **9c**, all these benzimidazole derivatives resulted in a nonmutagen profiling and **9a,d** as noncarcinogenic in rat and mouse.

4 | CONCLUSIONS

To sum up, we discovered a new class of 1,2-substituted-1*H*-benzo[d]imidazole derivatives (i.e. **9a–d**) acting as non-covalent and selective inhibitors of the *L. mexicana* cysteine protease CPB2.8 Δ CTE, one of the most promising target within anti-*Leishmania* drug design. Overall, the most interesting compound turned out to be **9d** which showed affinity toward the enzyme in the submicromolar range ($K_i = 0.69 \mu\text{M}$) and activity in vitro against the intracellular form of the parasite (amastigotes of *L. infantum*) in the micromolar range ($\text{IC}_{50} = 6.8 \mu\text{M}$). Moreover, preliminary in silico ADME-Tox

studies indicated that **9d** exhibits a good oral availability and results in a nonmutagen and noncarcinogenic profiling. Taking together, these outcomes make **9d** a new lead structure for further drug design of anti-*Leishmania* agents.

ACKNOWLEDGMENTS

Free academic license from ChemAxon for its suite of programs is gratefully acknowledged.

CONFLICT OF INTEREST

The authors declare no competing financial interest.

ORCID

Antonio Rescifina  <http://orcid.org/0000-0001-5039-2151>

Nicola Micale  <http://orcid.org/0000-0002-9294-6033>

REFERENCES

- [1] WHO. A global brief on vector-borne diseases **2014**. http://apps.who.int/iris/bitstream/10665/111008/1/WHO_DCO_WHD_2014.1_eng.pdf
- [2] H. W. Murray, J. D. Berman, C. R. Davies, N. G. Saravia, *Lancet* **2005**, 366, 1561.
- [3] J. N. Sangshetti, F. A. K. Khan, A. A. Kulkarni, R. Arote, R. H. Patil, *RSC Adv.* **2015**, 5, 32376.
- [4] S. Khan, I. Khan, P. M. S. Chauhan, *Chem. Biol. Interface* **2015**, 5, 1.
- [5] G. H. Coombs, J. C. Mottram, *Parasitology* **1997**, 114, S61.
- [6] P. A. Casgrain, C. Martel, W. R. McMaster, J. C. Mottram, M. Olivier, A. Descoteaux, *PLoS Pathog.* **2016**, 12, e1005658.
- [7] W. A. S. Wagner Judice, L. Puzer, S. S. Cotrin, A. K. Carmona, G. H. Coombs, L. Juliano, M. A. Juliano, *Eur. J. Biochem.* **2004**, 271, 1046.
- [8] K. Steert, I. El-Sayed, P. Van der Veken, A. Krishtal, C. Van Alsenoy, G. D. Westrop, J. C. Mottram, G. H. Coombs, K. Augustyns, A. Haemers, *Bioorg. Med. Chem. Lett.* **2007**, 17, 6563.
- [9] K. Steert, M. Berg, J. C. Mottram, G. D. Westrop, G. H. Coombs, P. Cos, L. Maes, J. Joossens, P. Van der Veken, A. Haemers, K. Augustyns, *ChemMedChem* **2010**, 5, 1734.
- [10] A. Ponte-Sucre, R. Vicik, M. Schultheis, T. Schirmeister, H. Moll, *Antimicrob. Agents Chemother.* **2006**, 50, 2439.
- [11] U. Schurigt, C. Schad, C. Glowa, U. Baum, K. Thomale, J. K. Schnitzer, M. Schultheis, N. Schaschke, T. Schirmeister, H. Moll, *Antimicrob. Agents Chemother.* **2010**, 54, 5028.
- [12] C. Schad, U. Baum, B. Frank, U. Dietzel, F. Mattern, C. Gomes, A. Ponte-Sucre, H. Moll, U. Schurigt, T. Schirmeister, *Antimicrob. Agents Chemother.* **2016**, 60, 797.
- [13] J. Schröder, S. Noack, R. J. Marhöfer, J. C. Mottram, G. H. Coombs, P. M. Selzer, *PLoS ONE* **2013**, 8, e77460.
- [14] V. S. Gontijo, W. A. Judice, B. Codonho, I. O. Pereira, D. M. Assis, J. P. Januário, E. E. Caroselli, M. A. Juliano, A. de Carvalho Dosatti, M. J. Marques, C. Viegas Jr, M. Henrique dos Santos, *Eur. J. Med. Chem.* **2012**, 58, 613.

- [15] L. R. de Sousa, H. Wu, L. Nebo, J. B. Fernandes, M. F. da Silva, W. Kiefer, T. Schirmeister, P. C. Vieira, *Exp. Parasitol.* **2015**, *156*, 42.
- [16] A. Scala, N. Micale, A. Piperno, A. Rescifina, T. Schirmeister, J. Kesselring, G. Grassi, *RSC Adv.* **2016**, *6*, 30628.
- [17] L. Massai, L. Messori, N. Micale, T. Schirmeister, L. Maes, D. Fregona, M. A. Cinellu, C. Gabbiani, *Biometals* **2017**, *30*, 313.
- [18] A. Scala, A. Rescifina, N. Micale, A. Piperno, T. Schirmeister, L. Maes, G. Grassi, *Chem. Biol. Drug Des.* **2017**, *91*, 597.
- [19] G. Chakrabarti, A. Basu, P. P. Manna, S. B. Mahato, N. B. Mandal, S. Bandyopadhyay, *J. Antimicrob. Chemother.* **1999**, *43*, 359.
- [20] F. Pagniez, H. Abdala-Valencia, P. Marchand, M. Le Borgne, G. Le Baut, S. Robert-Piessard, P. Le Pape, *J. Enzyme Inhib. Med. Chem.* **2006**, *21*, 277.
- [21] J. C. Tanaka, C. C. da Silva, I. C. Ferreira, G. M. Machado, L. L. Leon, A. J. de Oliveira, *Phytomedicine* **2007**, *14*, 377.
- [22] M. Taha, N. H. Ismail, M. Ali, K. M. Khan, W. Jamil, S. M. Kashif, M. Asraf, *Med. Chem. Res.* **2014**, *23*, 5282.
- [23] S. Pandey, S. S. Chauhan, R. Shivahare, A. Sharma, S. Jaiswal, S. Gupta, J. Lal, P. M. S. Chauhan, *Eur. J. Med. Chem.* **2016**, *110*, 237.
- [24] A. Scala, M. Cordaro, G. Grassi, A. Piperno, G. Barberi, A. Cascio, F. Risitano, *Bioorg. Med. Chem.* **2014**, *22*, 1063.
- [25] M. B. Félix, E. R. de Souza, M. D. C. A. de Lima, D. K. G. Frade, V. L. Serafim, K. A. D. F. Rodrigues, P. L. D. N. Nériss, F. F. Ribeiro, L. Scotti, M. T. Scotti, T. M. de Aquino, F. J. B. Mendonça Junior, M. R. de Oliveira, *Bioorg. Med. Chem.* **2016**, *24*, 3972.
- [26] A. M. Monforte, S. Ferro, L. De Luca, G. Lo Surdo, F. Morreale, C. Pannecouque, J. Balzarini, A. Chimirri, *Bioorg. Med. Chem.* **2014**, *22*, 1459.
- [27] S. Ferro, M. R. Buemi, L. De Luca, F. E. Agharbaoui, C. Pannecouque, A. M. Monforte, *Bioorg. Med. Chem.* **2017**, *25*, 3861.
- [28] M. R. Buemi, L. De Luca, S. Ferro, E. Russo, G. De Sarro, R. Gitto, *Bioorg. Med. Chem.* **2016**, *24*, 1513.
- [29] M. R. Buemi, L. De Luca, S. Ferro, R. Gitto, *Arch. Pharm.* **2014**, *347*, 533.
- [30] R. Gitto, L. De Luca, S. Ferro, E. Russo, G. De Sarro, M. Chisari, L. Ciranna, J. Alvarez-Builla, R. Alajarin, M. R. Buemi, A. Chimirri, *Bioorg. Med. Chem.* **2014**, *22*, 1040.
- [31] R. Gitto, L. De Luca, S. Ferro, A. Scala, S. Ronsisvalle, C. Parenti, O. Prezzavento, M. R. Buemi, A. Chimirri, *Bioorg. Med. Chem.* **2014**, *22*, 393.
- [32] M. R. Buemi, L. De Luca, A. Chimirri, S. Ferro, R. Gitto, J. Alvarez-Builla, R. Alajarin, *Bioorg. Med. Chem.* **2013**, *21*, 4575.
- [33] A. M. Monforte, L. De Luca, M. R. Buemi, F. E. Agharbaoui, C. Pannecouque, S. Ferro, *Bioorg. Med. Chem.* **2018**, *26*, 661.
- [34] S. J. Sanderson, K. G. J. Pollock, J. D. Hilley, M. Meldal, P. S. T. Hilaire, M. A. Juliano, L. Juliano, J. C. Mottram, G. H. Coombs, *Biochem. J.* **2000**, *347*, 383.
- [35] R. Kuhelj, M. Dolinar, J. Pungercar, V. Turk, *Eur. J. Biochem.* **1995**, *229*, 535.
- [36] R. Vicik, M. Busemann, C. Gelhaus, N. Stiefl, J. Scheiber, W. Schmitz, F. Schulz, M. Mladenovic, B. Engels, M. Leippe, K. Baumann, T. Schirmeister, *ChemMedChem* **2006**, *1*, 1126.
- [37] C. E. Mowbray, S. Braillard, W. Speed, P. A. Glossop, G. A. Whitlock, K. R. Gibson, J. E. J. Mills, A. D. Brown, J. M. F. Gardner, Y. F. Cao, W. Hua, G. L. Morgans, P. B. Feijens, A. Matheussen, L. J. Maes, *J. Med. Chem.* **2015**, *58*, 9615.
- [38] A. R. Allouche, *J. Comput. Chem.* **2011**, *32*, 174.
- [39] J. J. P. Stewart, *J. Mol. Mod.* **2007**, *13*, 1173.
- [40] J. J. P. Stewart, MOPAC2016, Stewart Computational Chemistry, Colorado Springs, CO **2016**.
- [41] E. Krieger, YASARA, Biosciences GmbH, Vienna, Austria **2013**.
- [42] E. Krieger, J. E. Nielsen, C. A. E. M. Spronk, G. Vriend, *J. Mol. Graph. Model.* **2006**, *25*, 481.
- [43] W. D. Cornell, P. Cieplak, C. I. Bayly, I. R. Gould, K. M. Merz, D. M. Ferguson, D. C. Spellmeyer, T. Fox, J. W. Caldwell, P. A. Kollman, *J. Am. Chem. Soc.* **1995**, *117*, 5179.
- [44] Y. Duan, C. Wu, S. Chowdhury, M. C. Lee, G. M. Xiong, W. Zhang, R. Yang, P. Cieplak, R. Luo, T. Lee, J. Caldwell, J. M. Wang, P. Kollman, *J. Comput. Chem.* **2003**, *24*, 1999.
- [45] U. Essmann, L. Perera, M. L. Berkowitz, T. Darden, H. Lee, L. G. Pedersen, *J. Chem. Phys.* **1995**, *103*, 8577.
- [46] A. Jakalian, D. B. Jack, C. I. Bayly, *J. Comput. Chem.* **2002**, *23*, 1623.
- [47] E. Krieger, R. Dunbrack, R. Hooft, B. Krieger, *Comput. Drug Discov. Des.* **2012**, *819*, 405.
- [48] R. W. W. Hooft, G. Vriend, C. Sander, E. E. Abola, *Nature* **1996**, *381*, 272.
- [49] A. Pedretti, L. Villa, G. Vistoli, *J. Comput. Aided Mol. Des.* **2004**, *18*, 167.
- [50] G. M. Morris, R. Huey, W. Lindstrom, M. F. Sanner, R. K. Belew, D. S. Goodsell, A. J. Olson, *J. Comput. Chem.* **2009**, *30*, 2785.
- [51] M. L. Barreca, A. Rao, L. De Luca, N. Iraci, A. M. Monforte, G. Maga, E. De Clercq, C. Pannecouque, J. Balzarini, A. Chimirri, *Bioorg. Med. Chem. Lett.* **2007**, *17*, 1956.
- [52] A. M. Monforte, A. Rao, P. Logoteta, S. Ferro, L. De Luca, M. L. Barreca, N. Iraci, G. Maga, E. De Clercq, C. Pannecouque, A. Chimirri, *Bioorg. Med. Chem.* **2008**, *16*, 7429.
- [53] W. X. Tian, C. L. Tsou, *Biochemistry* **1982**, *21*, 1028.
- [54] P. Cos, A. J. Vlietinck, D. V. Berghe, L. Maes, *J. Ethnopharmacol.* **2006**, *106*, 290.
- [55] J. C. Powers, J. L. Asgian, O. D. Ekici, K. E. James, *Chem. Rev.* **2002**, *102*, 4639.
- [56] A. L. Hopkins, C. R. Groom, A. Alex, *Drug Discov. Today* **2004**, *9*, 430.
- [57] A. L. Hopkins, G. M. Keseru, P. D. Leeson, D. C. Rees, C. H. Reynolds, *Nat. Rev. Drug Discov.* **2014**, *13*, 105.
- [58] G. Lauro, M. Masullo, S. Piacente, R. Riccio, G. Bifulco, *Bioorg. Med. Chem.* **2012**, *20*, 3596.
- [59] G. Lauro, A. Romano, R. Riccio, G. Bifulco, *J. Nat. Prod.* **2011**, *74*, 1401.
- [60] T. I. Oprea, A. M. Davis, S. J. Teague, P. D. Leeson, *J. Chem. Inf. Comput. Sci.* **2001**, *41*, 1308.

SUPPORTING INFORMATION

Additional supporting information may be found online in the Supporting Information section at the end of the article.

How to cite this article: De Luca L, Ferro S, Buemi MR, et al. Discovery of benzimidazole-based *Leishmania mexicana* cysteine protease CPB2.8ΔCTE inhibitors as potential therapeutics for leishmaniasis. *Chem Biol Drug Des.* 2018;92:1585–1596.
<https://doi.org/10.1111/cbdd.13326>